CHEMISTRY
A EUROPEAN JOURNAL

DOI: 10.1002/chem.200500588

Hollow Silica Spheres with an Ordered Pore Structure and Their Application in Controlled Release Studies

Nicole E. Botterhuis,[a] Qianyao Sun,[a] Pieter C. M. M. Magusin,[b] Rutger A. van Santen,[b] and Nico A. J. M. Sommerdijk*[a]

Abstract: Herein we report the synthesis and characterization of hollow silica spheres with a narrow size distribution, uniform wall thickness, and a wormlike pore structure. The formation of these spheres was monitored by confocal laser scanning microscopy and dynamic light scattering. A model for the molecular build-up of these silica hollow spheres is derived from these data in combination with studies of the as-made particles by transmission electron microscopy, scanning electron microscopy, pore size analysis, thermogravimetric analysis, and solid-state nuclear magnetic resonance. We further demonstrate that these spheres can be used for the encapsulation and subsequent release of different dye molecules.

Keywords: biomimetic mineralization · block copolymers · materials science · mesoporous materials · template synthesis

Introduction

The silica exoskeleton of diatoms is an intriguing example of the mineralized structures that provide support and protection to a large range of organisms. This mesostructured inorganic matrix with a hierarchical morphology is formed by deposition of amorphous polysilicic acid on the outer wall of the diatom. This process is regulated by organic templates that are produced by the diatoms themselves.[1] These low-density, thermally and mechanically stable materials have attracted the attention of chemists and materials scientists for their potential use in a variety of applications such as enzyme immobilization,[2] thermal and electronic insulators, catalysts, sorbents, controlled drug-delivery agents, and biomolecular separators.[3]

Highly ordered mesoporous synthetic silicas—MCM-type materials—were first synthesized by using the ionic surfactant cetyltrimethylammonium bromide (CTAB) as a structure-directing agent.[4] Later, it was shown that nonionic surfactants can also serve as templating agents for the formation of mesoporous silicas with varying pore morphologies and different pore sizes.[5] These findings opened-up a new field in which different lyotropic phases of a large variety of surfactants and amphiphilic polymers have been used to structure the developing silica phase that grows around these self-assembled organic templates to form numerous new mesophases.[6] At present, mesoporous silicas with controlled morphology are receiving increasing attention for their potential applications as compartments for the storage and release of (bio)molecules.

Silica hollow spheres have been prepared by templating routes that make use of vesicles,[7,8] solid particles,[9,10] and emulsion systems,[11,12] but also by the use of acoustic cavitation[13] or electrically forced liquid jets.[14] However, among these only a few examples of hollow spheres with an ordered wall structure exist.[7,11–13] The system developed in our laboratory[12] makes use of an emulsion of trimethylbenzene (TMB) in water, stabilized by a pluronic-type (*b*-poly(ethylene oxide)-*b*-poly(propylene oxide)-*b*-poly(ethylene oxide)) triblock copolymer ($\mathbf{EO_{76}}$-$\mathbf{PO_{29}}$-$\mathbf{EO_{76}}$). These spheres, prepared at 80 °C, possess a well-defined, layered shell structure (average diameter: 1000 nm; thickness: ~100 nm) that consists of highly cross-linked silica.

Many systems have been proposed in the literature for drug delivery. These include, for example, oil dispersions, liposomes, low-density lipoproteins, polymeric micelles, hydrophilic drug–polymer complexes, silica–poly(NIPAAm)

[a] N. E. Botterhuis, Dr. Q. Sun, Dr. N. A. J. M. Sommerdijk
Laboratory of Macromolecular and Organic Chemistry
Eindhoven University of Technology
P.O. Box 513, 5600 MB Eindhoven (The Netherlands)
Fax: (+31) 40-245-1036
E-mail: n.sommerdijk@tue.nl

[b] Dr. P. C. M. M. Magusin, Prof. Dr. R. A. van Santen
Schuit Institute of Catalysis
Eindhoven University of Technology
P.O. Box 513, 5600 MB Eindhoven (The Netherlands)

hybrid gels,[15] porous silica xerogels,[16] calcium phosphate nanoparticles,[17] drug nanoparticles encapsulated in macromolecular nanoshells,[18] or silica spheres.[19] The use of hollow silica spheres as controlled-release systems has often been suggested.[10] The hollow nature of the spheres makes them particularly suitable for controlled release as the distance of the individual encapsulated molecules to the particle surface is more homogeneous for hollow than for solid spheres. Furthermore, silica has been demonstrated to be a bio-inert but degradable material.[20] However, to the best of our knowledge only one example is known of the use of silica hollow spheres as a drug-delivery system.[10] This example involves post-synthesis drug loading and release. In this paper, however, we report the synthesis and characterization of dye-encapsulating hollow silica spheres. These spheres have a narrow size distribution, uniform wall thickness, and a worm-like pore structure. The synthesis temperature can be kept as low as 40 °C, which is compatible with the inclusion of delicate organic compounds. We also demonstrate that these spheres can indeed be used for the release of dye molecules.

Results and Discussion

Synthesis: The silica hollow spheres were synthesized by adding an ethanolic solution of 1,3,5-trimethylbenzene (TMB) to a solution of **EO_{76}-PO_{29}-EO_{76}** in 0.14 M HCl. Sodium silicate was then added to the resulting emulsion and the pH value was adjusted to 5.2. This mixture was aged for 4 h at 40 °C in closed containers without stirring, after which the silica particles were collected by filtration, washed, and subsequently freeze-dried.[21]

Starting from 1.0 g of **EO_{76}-PO_{29}-EO_{76}** and 0.68 g of SiO_2, 0.7 g of material was obtained, which corresponds to a yield of 42 %. Calcination at 700 °C reduced the sample to 70 % of its original weight, which indicates that the as-made samples contain approximately 30 wt % of the polymer. From this we calculated that 72 % of the sodium silicate and 21 % of the block copolymer had been incorporated in the spheres. These numbers were confirmed by thermogravimetric analysis (TGA) of both the samples and the dried filtrate and washing fluid.

Particle morphology: Scanning electron microscopy (SEM) showed that the obtained silica samples indeed consisted of spherical particles with a smooth surface and a size distribution of between 0.6 and 1.2 μm. The hollow nature of the particles was indicated by the observation of a small fraction of spheres (approximately 1 %) that were cracked (Figure 1 a).

This conclusion was confirmed by transmission electron microscopy (TEM), from which a shell thickness of 60–100 nm could also be derived. Significantly, TEM revealed a worm-like morphology within the particle shell that was interpreted as originating from organic channels (diameters of 3–5 nm) in a (more electron opaque) silica matrix that are oriented both parallel and perpendicular to the particle surface (Figure 1 b).

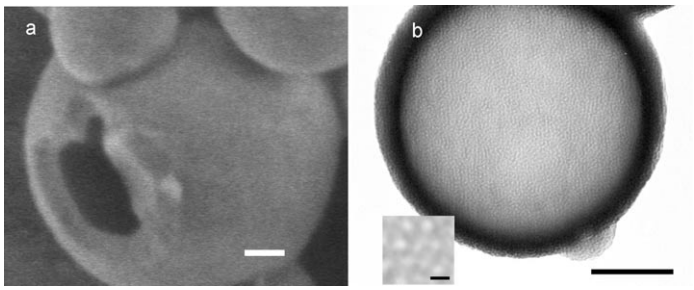

Figure 1. a) SEM image of a cracked particle, revealing its hollow nature and wall thickness. b) TEM image of as-made silica hollow spheres, revealing the porous structure of the spheres. Scale bars represent 200 nm. Inset: Magnification of the TEM image of the pores in the silica shell. Scale bar represents 7.5 nm.

As an approximation for the worm-like structure of the pores we use a simplified model in which the particle shell is represented as consisting of packed organic cylinders in a polymer/silica matrix (Figure 2). The pore volume/wall volume ratio A_{pores}/A_{wall} can be calculated by using the triangular unit cell and the values $d_1 = 3.5$ nm and $d_2 = 7.5$ nm determined from the TEM images (Figure 1 b).

$$A_{pores} = \frac{1}{2}\cdot\frac{\pi {d_1}^2}{4},\ A_{unit\ cell} = \left(\frac{1}{2}\cdot d_2\right)\cdot\left(\sqrt{3}\cdot\frac{1}{2}\cdot d_2\right) = \frac{\sqrt{3}}{4}\cdot {d_2}^2$$

$$A_{pores}/A_{wall} = \left(\frac{1}{2}\cdot\frac{\pi {d_1}^2}{4}\right)/\left(\left(\frac{\sqrt{3}}{4}\cdot {d_2}^2\right)-\left(\frac{1}{2}\cdot\frac{\pi {d_1}^2}{4}\right)\right)$$

From this calculation, a pore volume/wall volume ratio of 1/4 can be estimated. The volumetric polymer/SiO_2 ratio of 1/5 that was obtained from the TGA experiments[22] suggests that the polymer fraction is not large enough to account for the total pore volume. From this, and the fact that part of the PEO will also be entrapped in the silica matrix,[23] it follows that in the as-prepared particles a part of the pore volume must consist of TMB.

Pore size analysis: For the noncalcined, freeze-dried samples, pore size analysis by N_2 adsorption indicated a BET surface area of 3.6 $m^2 g^{-1}$ and a total pore volume of only 0.011 $cm^3 g^{-1}$.[24] This pore volume probably corresponds to the volume of the TMB that is included in the pores before freeze-drying. In contrast, for samples calcined at 550 °C for 4 h, a BET surface area of 430 $m^2 g^{-1}$ was determined. The total pore volume was measured to be 0.12 $cm^3 g^{-1}$, which corresponds to a relative pore volume of 19 %,[22] a number that is in good agreement with the pore volume/wall volume ratio estimated from the TEM images, and hence shows the validity of the model described above (Figure 2). A pore diameter of 3.5 nm was deduced, which again is in good agreement with the TEM observations.

The drastic increase in pore volume upon calcination was attributed to the formation of pores by the decomposition

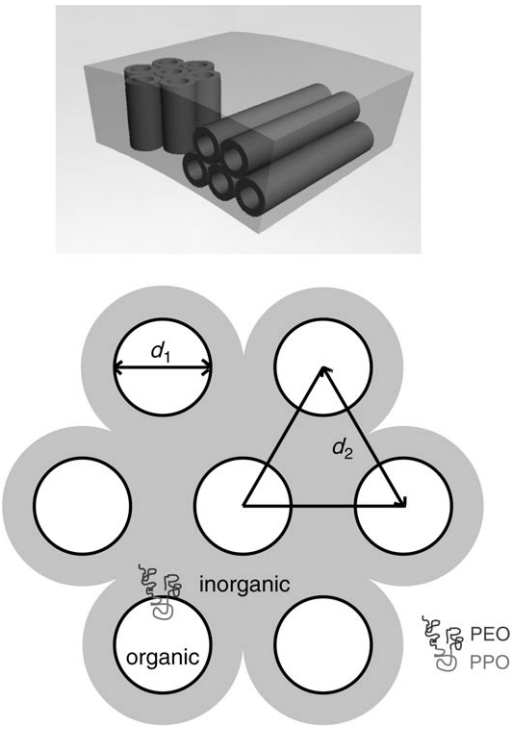

Figure 2. Schematic model of close-packed organic cylinders in a silica matrix. The unit cell that is used for the estimation of the pore volume/wall volume ratio is indicated with a triangle. The values for d_1 and d_2 can be estimated from the TEM image in Figure 1b.

of the organic phase, that is, of the **EO_{76}-PO_{29}-EO_{76}**. Interestingly, SEM revealed that the surface of the calcined particles was significantly rougher than that of the noncalcined particles (Figure 3). This was attributed to the rupture of the outermost silica layer by escaping combustion products.

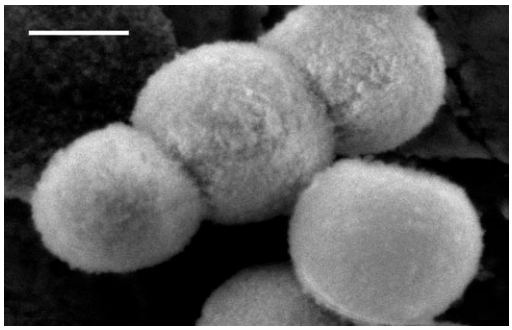

Figure 3. SEM image of silica hollow spheres after calcination. The scale bar represents 500 nm.

Solid-state NMR spectroscopy: To investigate the supramolecular structure of the particles by magic angle spinning (MAS) ^{1}H NMR spectroscopy without the normally overwhelming presence of the H_2O signal, the samples were prepared in D_2O. They were also only partially dried after synthesis, by which means well-resolved TMB resonances could be observed in the ^{1}H NMR spectra. In addition to centerband signals with shift values close to those in the solution spectra, the 4 kHz MAS ^{1}H NMR spectra show small but significant sample-rotation sidebands (Figure 4). The origin of these sidebands could be residual ^{1}H–^{1}H dipole couplings as a result of nonisotropic rotational motion, or local susceptibility effects. Consequently, trapped or adsorbed solvent molecules with a sufficiently long residence time tend to have more intense sidebands than solvent molecules tumbling freely in solution. Interestingly, the spinning sidebands of the TMB peaks in the ^{1}H NMR spectrum consist of a sharp ($\delta = 9.9$ ppm) and a broad ($\delta = 9.75$ ppm) component. We attribute this to the existence of two TMB phases: a

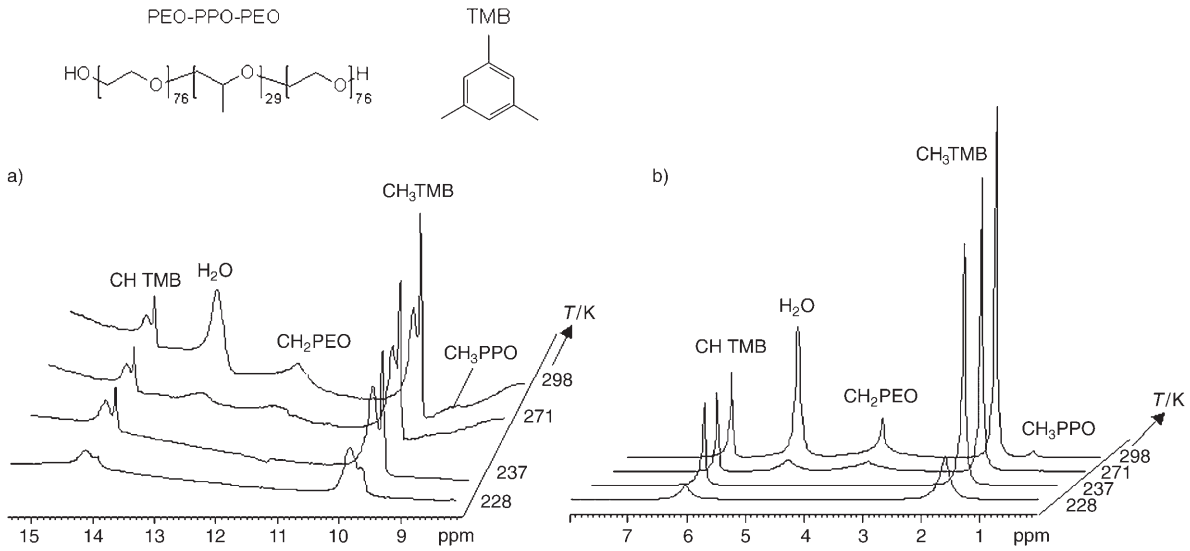

Figure 4. Variable-temperature ^{1}H NMR spectra of particles that were prepared in D_2O and were only partially dried after synthesis. a) First-order sideband region magnified 50 times. b) Centerband region corresponding to the typical shift values in liquid-state NMR spectroscopy.

bulk component with molecules tumbling isotropically in a homogeneous environment, and a surface-affected component that has a solid-like behavior, respectively.[25] Two-dimensional exchange ^{1}H NMR spectroscopy revealed cross-peak intensity between the resonances of the two phases of TMB for mixing times of 10 ms or longer. This indicates that TMB molecules can migrate between the mobile bulk phase and the relatively immobile surface-affected phase.[26]

Upon cooling the sameple, the MAS ^{1}H NMR signals of PPO, PEO, and water show strong broadening at 271 K (calibrated temperature), corresponding to the freezing point of water in mesopores (Figure 4). No significant changes, however, were observed in the ^{1}H NMR signals of TMB between 298 and 271 K. This indicates that the bulk fluid phase of TMB is not physically mixed with either the block copolymer or water, which is consistent with our model. The TMB resonances are strongly broadened at 228 K, that is, close to the freezing point of TMB. The broadening of the broad component in the spinning sideband of the TMB signal, assigned to the surface-affected fraction, is less dramatic than for the sharp component, which is related to the bulk phase. A likely explanation is melting point depression, as commonly found for molecules confined in a small volume.[27] This confirms our picture of a confined TMB phase located inside the mesopores of the particle shell.

The magic angle spinning ^{29}Si NMR line-shape could be deconvoluted into three gaussian components at $\delta = -92$, -102, and -111 ppm. These components were assigned to silicon with different numbers of Si neighbors in the second coordination sphere, namely $Q^2[Si(OSi)_2(OH)_2]$, Q^3 $[Si(OSi)_3(OH)_1]$, and Q^4 $[Si(OSi)_4]$, respectively. A Q^3/Q^4 ratio of 1.1 was determined from the line-shape deconvolution (repetition time 120 s, Figure 5a). This reflects a relatively low degree of cross linking at this synthesis temperature.

The cross-polarization-based ^{1}H–^{29}Si correlation NMR spectra[28] showed that all silica centers had short-range dipolar couplings with water. Apparently, water is well dispersed inside the silica matrix (Figure 5b). In ^{1}H–^{29}Si correlation NMR experiments extended with a spin-diffusion step of 300 ms[29] we readily observed cross-peaks between the PEO resonances and the three silica signals. This confirms the inclusion of the PEO in the silica matrix (Figure 5c). Two-dimensional exchange ^{1}H NMR spectra recorded with a dipolar mixing time of 10 ms showed evidence of short-range (<5 Å) dipolar couplings between the water and PEO protons, whereas the cross-peaks between the water and PPO methyl protons could only be observed at high mixing times (300 ms). This suggests that only the PEO blocks are directly in contact with the water included in the silica matrix.

A comparison of the MAS ^{13}C NMR spectra of the partially dried particles with those of lyophilized silica particles demonstrated that TMB is successfully removed by the freeze-drying process (not shown). This is important for the potential application of these particles as a drug-delivery device.

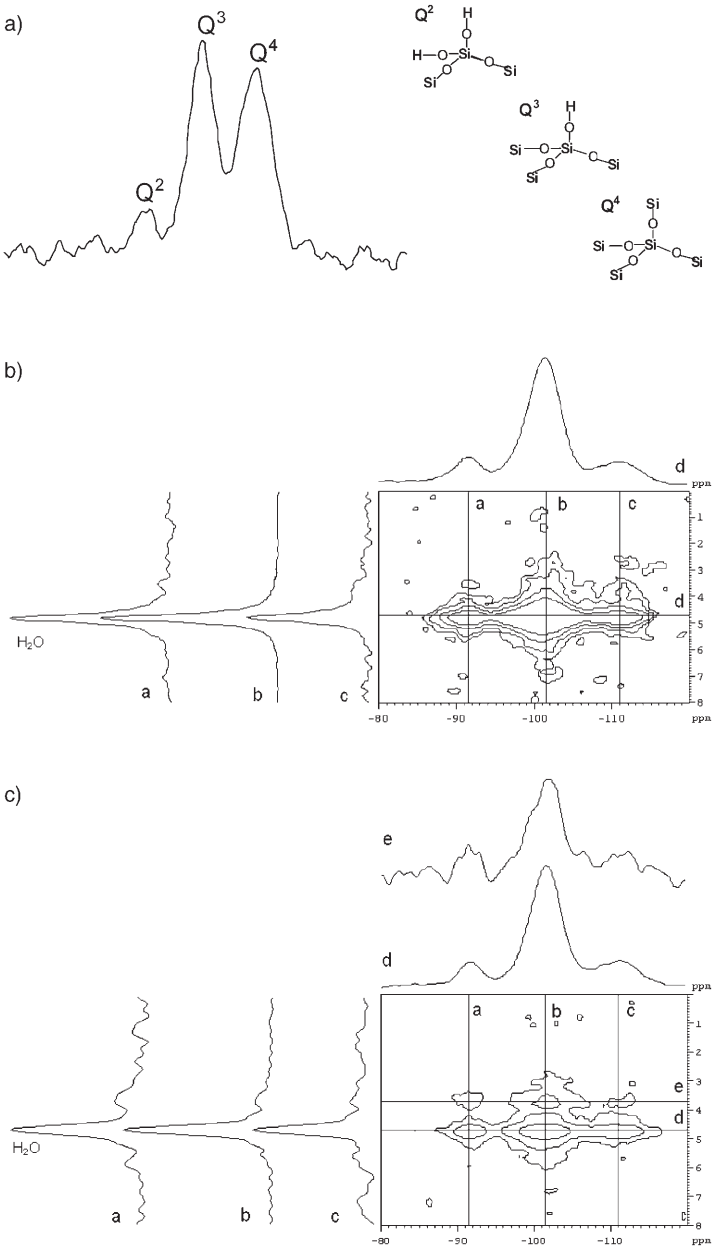

Figure 5. a) ^{29}Si MAS NMR spectrum of as-made silica particles. The ratio between the peak areas of Q^3 and Q^4 is a measure of the degree of cross-linking of the silica network. b) and c) ^{1}H-^{29}Si correlation NMR spectra of partially dried silica particles prepared in D_2O. Lines **a**–**e** indicate cross-sections trough the 2D spectrum (**a**: Q^2, **b**: Q^3, **c**: Q^4, **d**: H_2O, **e**: CH_2 PEO). In c), the experiment is extended with a spin diffusion step.

Monitoring particle formation: To get insight into the mechanism of the formation of the silica hollow spheres, the different stages in the synthesis were monitored by confocal laser scanning microscopy (CLSM). To this end, Eosin B Spirit Soluble (ES), a fluorescent dye, was added to the TMB/EtOH mixture prior to mixing it with the acidified aqueous PEO-PPO-PEO solution. The fluorescence micrographs revealed that the size of the emulsion droplets is of the order of 200 nm (Figure 6a). Upon addition of the

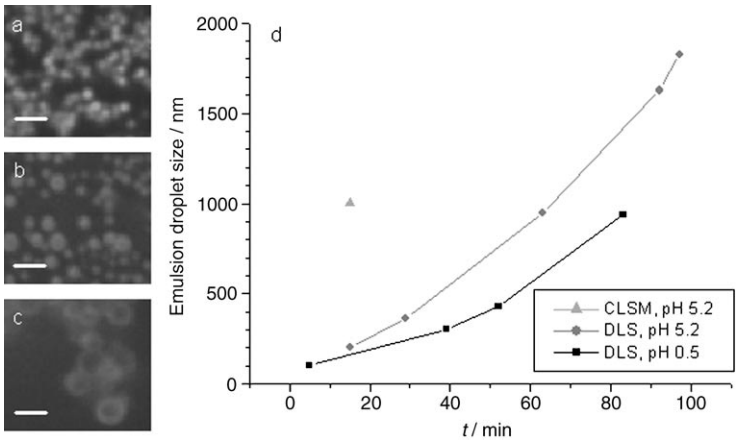

Figure 6. a)–c) CLSM pictures of Eosin B-containing particles at different stages of synthesis. Scale bars represent 1 μm. a) Emulsion droplets of TMB with PEO-PPO-PEO in water (pH ~ 0.5). b) After addition of sodium silicate (pH ~ 2). c) After addition of NaOH (pH ~ 5.2). d) Dependence of average emulsion droplet size on pH and time as determined by DLS (■ and ●) and CLSM (▲) analysis of the sample presented in c.

sodium silicate solution the size of these droplets increased only slightly to 200–300 nm (Figure 6b); however, upon raising the pH to 5.2 CLSM revealed that particles with an average size of 1 μm and a fluorescent shell of about 100 nm were predominant within 15 minutes (Figure 6c).

This increase in size, in contrast to earlier beliefs, argues against a true templating role of the emulsion droplets. Dynamic light scattering (DLS) showed a gradual increase in the size of the emulsion droplets upon standing before mineralization (Figure 6d). It was further found that this process is faster at higher pH, and at a pH of 5.2, as used in the synthesis procedure, an average emulsion droplet size of 1000 nm was reached after 1 h. However, at pH 5.2 and in the presence of sodium silicate, this point was already reached after about 15 minutes, thereby suggesting that the interaction of the sodium silicate with the block copolymer plays a role in the increase in particle size. Hydrogen-bond formation between the silica precursor and $\mathbf{EO_{76}\text{-}PO_{29}\text{-}EO_{76}}$ most likely leads to a decreased emulsifying action of the block copolymer, which results in larger, but stable, emulsion droplets that subsequently become mineralized.

Dye encapsulation: To explore the possibility of using the hollow interior of these silica spheres as containers from which organic molecules can be released, dyes with different hydrophobicities were incorporated during the synthesis in a manner similar to that described above for Eosin. CSLM revealed that whereas all the dyes were contained in the initial emulsion droplets, the location of the dye in the silica particles depended on its specific hydrophobicity (Figure 7), that is, only the most hydrophobic ones (Sudan II (SII) and Quinoline Yellow (QY)) remained in the TMB phase after addition of the sodium silicate. In all other cases (Fluorexon(F), Rose Bengal (RB), and ES) the dyes were located in the outermost layer of the particles, most likely by entrapment in the developing silica shell.

The amount of dye that could be loaded into these silica spheres also depended on the hydrophilicity of the specific compounds. With TGA we compared the mass loss of the dye-containing spheres with the mass loss of the spheres which contained the block copolymer as the only organic component. Assuming a constant silica/block copolymer ratio we determined loadings ranging from around 2.5 to 15 wt% (with an error of ±2% for all dyes) for seven different dyes. The hydrophobic ones that were located in the central TMB phases could be loaded up to amounts

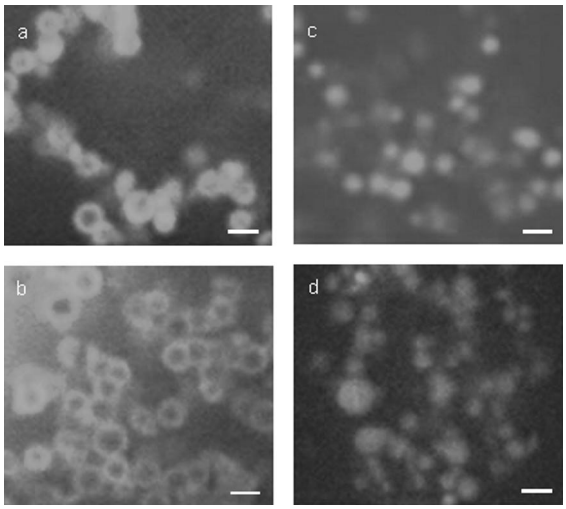

Figure 7. CLSM pictures of as-prepared silica particles with encapsulated dyes. Data bars represent 1 μm. a) Rose Bengal, b) Eosin B, c) Sudan II, and d) Quinoline Yellow.

of 4% (QY), 8.5% (SII), and 15% (Pyrene), whereas the hydrophilic dyes could only be loaded up to 2.5% (RB), 3.0% (ES), and 3.2% (F).

No dramatic effect in pore size due to the immobilization of the dye molecules was observed from BET analysis of the resulting materials, either before or after calcination (Figure 8). However, the surface area (552 $m^2 g^{-1}$) and pore volume (0.20 $cm^3 g^{-1}$) of the RB-containing spheres were significantly larger after calcination than those of the QY-containing particles (495 $m^2 g^{-1}$ and 0.14 $cm^3 g^{-1}$, respectively), which is only slightly higher than the values for the silica spheres without encapsulated dye. The difference between RB and QY may be due to the fact that RB is located in the shell of the particles, whereas QY is loaded in the core of the particles.

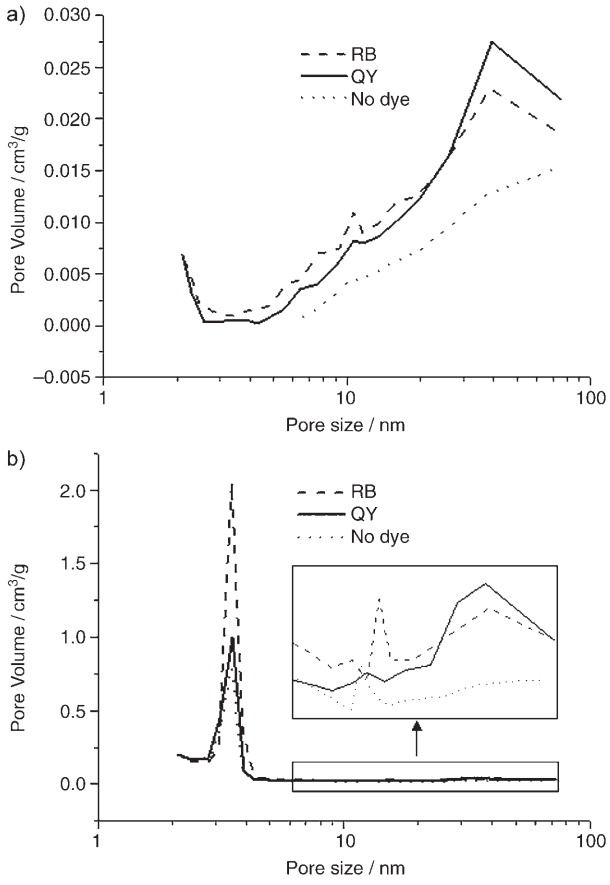

Figure 8. Pore size distributions in a) as-made samples and b) calcined silica spheres with and without incorporated dyes.

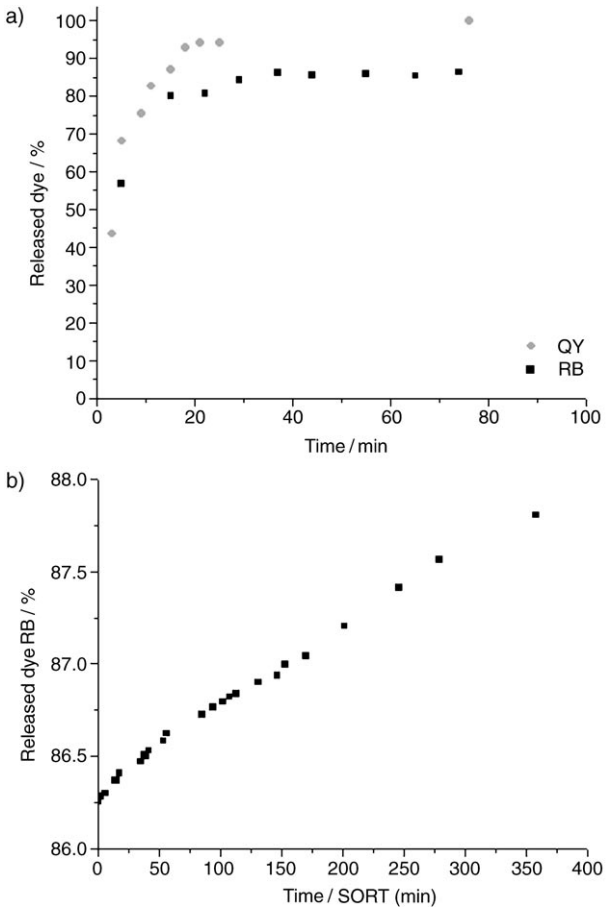

Figure 9. a) Release characteristics of freeze-dried silica spheres containing QY or RB dispersed in PBS at 37 °C. b) Second release from RB-containing silica spheres after rinsing and re-dispersion of the particles.

Release experiments: For a further study of the release of the encapsulated compounds from these spheres upon immersion in aqueous media we selected QY, one of the dyes that are located in the interior of the spheres. For this purpose a release experiment was performed in which a low amount of the freeze-dried, dye-containing particles was dispersed in phosphate-buffered saline (PBS, 10 mM phosphate and 0.9 wt. % NaCl in ultrapure water at pH 7.4) contained in a thermostatted (37 °C) shaking vessel. UV spectroscopy revealed a fast release in the first 20 minutes of the experiment, after which the release leveled off (Figure 9a).

When a release experiment was performed in a thermostatted (37 °C) shaking vessel with RB, a probe that is localized in the shell of the particles, a similarly fast release was observed to that for QY (Figure 9a). However, rather than leveling-off of the release after approximately 20 min, we observed a contribution of a new, although slower, release mechanism. This rate was linear with the square root of time for approximately three months, thus suggesting a stable, diffusion-controlled, release (Figure 9b).[30]

The difference in release rates may be explained by assuming two kinds of encapsulation states of the dye: in one state the dye may be immobilized in the meso- and macropores, from which it can easily diffuse out, whereas in the other state, which comprises only a small amount of the dye, it could be included in the silica walls, which must dissolve prior to release of the dye.

Interestingly, the dye molecules are able to escape from the particles despite the fact that the pore size analysis pointed to a very low surface area before the calcinations. This indicates that there is only a small amount of pores present in the particles. Nevertheless, a small amount of pores with diameters of 10 nm was always observed, both before and after calcination (Figure 8), which may be responsible for the release of the dyes.

Conclusion

We have demonstrated that silica spheres with a hollow morphology and a worm-like pore structure can be synthesized in which dye molecules can be incorporated and subsequently released in aqueous media. Important in our synthesis route are the moderate silica-formation temperature (40 °C), which we believe to be compatible with the inclusion of a large variety of organic molecules, and the freeze-drying process, which limits the amount of cracked particles to around 1 % and removes the TMB. The organic dye mol-

ecules can be introduced by dispersing them in the organic phase of the **EO_{76}-PO_{29}-EO_{76}** stabilized emulsion around which the silica shell is formed. Hydrophobic dyes are located predominantly in the TMB phase of the particles, whereas more hydrophilic dyes are concentrated in the silica shell. The inclusion of a fluorescent dye in these emulsion droplets has allowed monitoring of the formation process. This revealed that, in contrast to earlier beliefs, the particles are not formed by a true templating process. Instead, the complexation of the polymer chains with silicate ions induces an increase in the droplet size from approximately 200 nm to 1 μm, which eventually determines the particle size.

Furthermore, we have shown the successful encapsulation of hydrophobic and more hydrophilic organic molecules. A fast release was observed in the first 20 minutes of the experiment for both hydrophobic and hydrophilic dyes. For Rose Bengal, which is more hydrophilic, a second slow release was observed that persisted for three months.

The observed release characteristics of our silica hollow spheres, in combination with the fact that the particles after freeze-drying consist of only silica and a pluronic-type polymer and that both materials have been proven to be biocompatible in tests in vivo, make this system a promising candidate for a future controlled-release system.

Experimental Section

Materials: 1,3,5-Trimethylbenzene (mesitylene, 97%), Quinoline Yellow, spirit soluble (95%), Sudan II, and potassium phosphate, monobasic, p. a., were purchased from Acros Organics. Poly(ethylene glycol)-block-poly(propylene glycol)-block-poly(ethylene glycol) (av. M_n = 8400 g mol^{-1}), Fluorexon (indicator grade), Rhodamine B base (97%), and Eosin B, spirit soluble (95%), were purchased from Aldrich. Sodium silicate solution (27 wt.% SiO_2, 8 wt.% Na_2O, analytical grade), Hydrochloric acid (1 N), dipotassium hydrogen phosphate (anhydrous extra pure), sodium chloride (GR for analysis), and sodium hydroxide pellets (extra pure) were purchased from Merck. Ethanol (AR) was purchased from Biosolve Ltd., Bengal Rose B was purchased from Fluka, D_2O (99.9%) was purchased from Cambridge Isotope Laboratories Inc., hydrochloric acid (min. 37%) was purchased from Vel, and dialysis membranes of 12–14 kD were purchased from Spectrum laboratories. Ultrapure water was used with a constant quality of 17.6 Ωm.

Synthesis of the silica hollow spheres: The silica hollow spheres were synthesized as follows: **EO_{76}-PO_{29}-EO_{76}** (1 g) was first dissolved in ultrapure water (73 g) and 12 mL of 1 M HCl was added to this mixture whilst stirring. TMB (1 g) was dissolved in 25 g of ethanol, then the solution was added slowly to the copolymer solution whilst stirring. A milky emulsion formed immediately. Finally, 10 mL of fourfold diluted sodium silicate solution was added dropwise with vigorous stirring. The pH value was then adjusted to 5.2 with dilute NaOH solution (0.1 or 2 N). After 4 h of aging at 40 °C in closed containers without stirring, the particles were collected by filtration and washed with 500 mL of ultrapure water. The particles were dried either by rotation evaporation at 40 °C or freeze-drying; the latter method reduced the cracking to approximately 1% of the particles produced.

Dyes can be incorporated into the silica hollow spheres by replacing 10 wt.% of TMB with dye during the synthesis procedure, and dissolving the dye in the TMB and ethanol mixture before adding it to the acidified solution of PEO-PPO-PEO in water.

Confocal laser scanning microscopy (CLSM): Cross-sectional fluorescence images were recorded on a Perkin Elmer Ultraview LCI confocal imaging system in the spatial mode, which was connected to a Zeiss Axiovert 200 inverse microscope equipped with a 100× oil immersion objective with a numerical aperture of 1.4. An Omnichrome 643-life A01 ion laser was used as the excitation source. An excitation filter of 488 nm was used. Samples were prepared by placing a droplet of a suspension of particles in water between a microscope plate and a thin glass cover slip.

Magic angle spinning (MAS) NMR spectroscopy: All MAS NMR spectra were recorded on a Bruker DMX-500 spectrometer operating at ^{1}H, ^{13}C, and ^{29}Si NMR frequencies of 500, 125, and 99 MHz, respectively. Both a 4-mm and a 7-mm magic angle spinning (MAS) probe-head were used with sample rotation rates of 4 kHz. Hahn echoes were recorded by use of the 90°-τ-180°-τ two-pulse sequence with a delay, τ, of 2.5 μs and a 90° pulse of 5 μs. High-power (50 kHz) proton decoupling was used to remove the effect of dipolar ^{1}H-^{13}C and ^{1}H-^{29}Si broadening. The number of scans for the ^{13}C NMR spectra was 1024, and the relaxation delay 10 s. For quantitative ^{29}Si NMR hpdec spectra, 512 scans were accumulated with an interscan delay of 120 s to have full relaxation of all peaks. Cross-polarization from ^{1}H to ^{29}Si was recorded with a ramped contact pulse of 10 ms and an interscan delay of 3 s. The wideline-separated spectroscopy (WISE) pulse sequence[28] with ramped contact pulse was used to correlate the ^{1}H NMR resonances with those of the ^{13}C or ^{29}Si nuclei. For observing relayed ^{1}H–^{13}C and ^{1}H–^{29}Si contacts the WISE experiment was extended with a spin diffusion time interval before the cross polarization.[25] Finally, 2D exchange ^{1}H NMR spectra were recorded by use of the standard NOESY pulse sequence with three 90° pulses.

All NMR measurements were performed on samples that were synthesized in D_2O,[31] and either freeze-dried or only briefly dried at room temp. to prevent complete evaporation of TMB.

Scanning electron microscopy: SEM was performed on a Philips XL30 ESEM-FEG electron microscope in the hi-vac mode. The acceleration voltage used was either 2.0 or 3.0 kV. Samples were prepared by either placing a droplet of a suspension of the particles in ethanol on an aluminum stub and evaporation of the ethanol or by mounting the particles with carbon tape on an aluminum stub.

Transmission electron microscopy: TEM was performed using a JEOL JEM-2000FX electron microscope operating at 80 kV. Samples were mounted on copper–carbon grids by placing a droplet of a suspension of particles in water on the grid, and removing the water with filter paper after either 10 or 60 seconds.

Thermogravimetric analysis: TGA experiments were performed on a Pyris 6 thermogravimetric analyzer (Perkin Elmer). Samples were heated at a heating rate of 1 °C min^{-1} from 50 to 600 °C. The dye loading capacity of the particles was calculated by assuming that the ratio of PEO-PPO-PEO to silica, which can be calculated from TGA on a particle without dye, is the same in all the samples.

Pore size analysis: The distribution of pores was measured by the nitrogen adsorption method at liquid nitrogen temperature on a Tri-Star 2000 (Micromeritics Co.) using standard continuous procedures. Calcined samples were degassed for 4 h at 150 °C, while noncalcined samples were degassed for 15 h at 80 °C because at 150 °C the PEO-PPO-PEO starts to decompose, as was seen by TGA. The surface area was determined by the BET method in the 0.05–0.3 relative pressure range. The Barrett–Joyner–Halenda (BJH) method was used to analyze adsorption and desorption curves.[32] The values for surface area, pore volume, and pore-size distribution given above were calculated from the desorption branch of the isotherm plot.

Dynamic light scattering: Dynamic light scattering measurements were performed on a Malvern 7400 system with an Ion laser technology model 5400 laser (λ = 488 nm). The aperture was adjusted between 35 and 100 to have about the same number of counts per minute in each measurement. Samples were made by preparing an emulsion by the normal procedure, without addition of the sodium silicate, and dividing this emulsion into two beakers. In one of the beakers the pH was not adjusted, whereas in the other beaker the pH was immediately adjusted to 5.2 with an NaOH solution (2 N or 0.1 N). Samples were taken from these beakers alternately.

Release studies: For the experiments in shaking vessels, freeze-dried, dye-containing particles were suspended in phosphate-buffered saline (PBS, 10 mM phosphate and 0.9 wt. % NaCl in ultrapure water, pH 7.4; the amount of spheres corresponds to 0.1 w/v % for RB and 0.0046 w/v % for QY) and placed in a thermostatted beaker at 37 °C. For the particles containing the hydrophilic dye (RB), the suspension was filtered and washed after 400 minutes and the particles were re-suspended in 50 mL of buffer to further monitor the second release.

In another release experiment, dialysis was performed in an equilibrium dialyzer (Spectrum laboratories), in which five cells consisting of two Teflon-coated compartments of 6 mL, divided by a dialysis membrane of 12–14 kD, were rotated continuously in a water bath which was kept at a constant temperature of 37 °C. Freeze-dried, QY-containing particles (50 mg) were put in the left compartment together with 3.5 mL of PBS and the right compartment was filled with 5 mL of PBS. After three and seven days the right compartments were emptied and refilled with 5 mL of buffer. The release was stopped after nine days.

Acknowledgments

The authors would like to thank B. Mezari (Eindhoven University of Technology) for his assistance with the NMR experiments, D. J. M. van Beek (Eindhoven University of Technology) for her assistance with the DLS experiments, and W. K. Gerritsen (Eindhoven University of Technology) for his assistance with the TGA experiments.

[1] a) S. Mann, *Angew. Chem.* **2000**, *112*, 3532–3548; *Angew. Chem. Int. Ed.* **2000**, *39*, 3393–3406; b) N. Kröger, R. Deutzmann, M. Sumper, *Science* **1999**, *286*, 1129–1132; c) E. G. Vrieling, T. P. M. Beelen, R. A. van Santen, W. W. C. Gieskes, *Angew. Chem.* **2002**, *114*, 1613–1616; *Angew. Chem. Int. Ed.* **2002**, *41*, 1543–1546.

[2] Y. Wang, F. Caruso, *Chem. Mater.* **2005**, *17*, 953–961.

[3] K. J. C. van Bommel, J. H. Jung, S. Shinkai, *Adv. Mater.* **2001**, *13*, 1472–1476, and references therein.

[4] a) J. S. Beck, J. C. Vartuli, W. J. Roth, M. E. Leonowicz, C. T. Kresge, K. D. Schmitt, C. T.-W. Chu, D. H. Olson, E. W. Sheppard, S. B. McCullen, J. B. Higgins, J. L. Schlenker, *J. Am. Chem. Soc.* **1992**, *114*, 10834–10843; b) C. T. Kresge, M. E. Leonowicz, W. J. Roth, J. C. Vartuli, J. S. Beck, *Nature* **1992**, *359*, 710–712; c) H. P. Lin, Y. R. Cheng, C. Y. Mou, *Chem. Mater.* **1998**, *10*, 3772–3776.

[5] S. A. Bagshaw, E. Prouzet, T. J. Pinnavaia, *Science* **1995**, *269*, 1242–1244.

[6] a) D. Zhao, J. Feng, Q. Huo, N. Melosh, G. H. Fredrickson, B. F. Chmelka, G. D. Stucky, *Science* **1998**, *279*, 548–552; b) D. Zhao, Q. Huo, J. Feng, B. F. Chmelka, G. D. Stucky, *J. Am. Chem. Soc.* **1998**, *120*, 6024–6036; c) K. Flodström, H. Wennerström, C. V. Teixeira, H. Amenitsch, M. Lindén, V. Alfredsson, *Langmuir* **2004**, *20*, 10311–10316; d) A. Sayari, S. Hamoudi, *Chem. Mater.* **2001**, *13*, 3151–3168; e) V. T. John, B. Simmons, G. L. McPherson, A. Bose, *Curr. Opin. Colloid Interface Sci.* **2002**, *7*, 288–295; f) T. Sen, G. J. T. Tiddy, J. L. Casci, M. W. Anderson, *Chem. Mater.* **2004**, *16*, 2044–2054.

[7] a) S. S. Kim, W. Zhang, T. J. Pinnavaia, *Science* **1998**, *282*, 1302–1305; b) P. T. Tanev, T. J. Pinnavaia, *Science* **1996**, *271*, 1267–1269.

[8] a) D. Lootens, C. Vautrin, H. van Damme, T. Zemb, *J. Mater. Chem.* **2003**, *13*, 2072–2074; b) D. H. W. Hubert, M. Jung, P. M. Frederik, P. H. H. Bomans, J. Meuldijk, A. L. German, *Adv. Mater.* **2000**, *12*, 1286–1290.

[9] a) F. Caruso, R. A. Caruso, H. Möhwald, *Science* **1998**, *282*, 1111–1114; b) F. Caruso, *Chem. Eur. J.* **2000**, *6*, 413–419.

[10] J.-F. Chen, H.-M. Ding, J.-X. Wang, L. Shao, *Biomaterials* **2004**, *25*, 723–727.

[11] a) R. S. Underhill, A. V. Jovanovic, S. R. Carino, M. Varshney, D. O. Shah, D. M. Dennis, T. E. Morey, R. S. Duran, *Chem. Mater.* **2002**, *14*, 4919–4925; b) S. E. Friberg, C.-C. Yang, R. Goubran, R. E. Partch, *Langmuir* **1991**, *7*, 1103–1106; c) P. S. Singh, K. Kosuge, *Chem. Lett.* **1998**, 101–102; d) C. E. Fowler, D. Khushalani, S. Mann, *Chem. Commun.* **2001**, 2028–2029; e) C. Yu, B. Tian, J. Fan, G. D. Stucky, D. Zhao, *Chem. Lett.* **2002**, 62–63; f) A. Lind, B. Spliethoff, M. Lindén, *Chem. Mater.* **2003**, *15*, 813–818.

[12] Q. Sun, P. J. Kooyman, J. G. Grossmann, P. H. H. Bomans, P. M. Frederik, P. C. M. M. Magusin, T. P. M. Beelen, R. A. van Santen, N. A. J. M. Sommerdijk, *Adv. Mater.* **2003**, *15*, 1097–1100.

[13] R. K. Rana, Y. Mastai, A. Gedanken, *Adv. Mater.* **2002**, *14*, 1414–1418.

[14] G. Larsen, R. Velarde-Ortiz, K. Minchow, A. Barrero, I. G. Loscertales, *J. Am. Chem. Soc.* **2003**, *125*, 1154–1155.

[15] a) I. Roy, T. Y. Ohulchanskyy, H. E. Pudavar, E. J. Bergey, A. R. Oseroff, J. Morgan, T. J. Dougherty, P. N. Prasad, *J. Am. Chem. Soc.* **2003**, *125*, 7860–7865; b) J. Kreuter, *Colloidal Drug Delivery Systems*, Marcel Dekker, New York, **1994**; c) M. Yokoyama, T. Okano, *Adv. Drug Del. Rev.* **1996**, *21*, 77–80.

[16] a) K. Unger, H. Rupprecht, B. Valentin, W. Kircher, *Drug Dev. Ind. Pharm.* **1983**, *9*, 69–91; b) P. Kortesuo, M. Ahola, S. Karlsson, I. Kangasniemi, J. Kiesvaara, A. Yli-Urpo, *J. Biomed. Mater. Res.* **1999**, *44*, 162–167.

[17] H. T. Schmidt, B. L. Gray, P. A. Wingert, A. E. Ostafin, *Chem. Mater.* **2004**, *16*, 4942–4947.

[18] A. S. Zahr, M. de Villiers, M. V. Pishko, *Langmuir* **2005**, *21*, 403–410.

[19] a) P. Kortesuo, M. Ahola, M. Kangas, M. Jokinen, T. Leino, L. Vuorilehto, S. Laakso, J. Kiesvaara, A. Yli-Urpo, M. Marvola, *Biomaterials* **2002**, *23*, 2795–2801; b) C. Charnay, S. Bégu, C. Tourné-Péteilh, L. Nicole, D. A. Lerner, J. M. Devoisselle, *Eur. J. Pharm. Biopharm.* **2004**, *57*, 533–540; c) C. Barbé, J. Bartlett, L. Kong, K. Finnie, H. Q. Lin, M. Larkin, S. Calleja, A. Bush, G. Calleja, *Adv. Mater.* **2004**, *16*, 1959–1966.

[20] a) J. Wilson, G. H. Pigott, F. J. Schoen, L. L. Hensch, *J. Biomed. Mater. Res.* **1981**, *15*, 805–817; b) E. J. A. Pope, K. Braun, C. M. Peterson, *J. Sol-Gel Sci. Technol.* **1997**, *8*, 635–639.

[21] Freeze-drying instead of drying in the air (ref. 12) drastically reduced the occurrence of cracked particles to only 1 %. This is due to the fact that no capillary forces can occur in the mesopores upon freeze-drying. Also, when these particles were not freeze-dried ^{1}H NMR spectroscopy showed that washing with $CDCl_3$ leads to the extraction of TMB. However, no TMB could be detected upon washing the freeze dried samples with $CDCl_3$, thus suggesting its successful removal during the lyophilization process (see also solid-state NMR section).

[22] The density of silica is 1.9 g cm^{-3} and the specific volume of the block copolymer was estimated to be 0.21 cm^{3}g^{-1}, with an even volume distribution of the hydrophobic and the hydrophilic blocks.

[23] It is known that PEO can act as a template for silica formation: Q. Sun, E. G. Vrieling, R. A. van Santen, N. A. J. M. Sommerdijk, *Curr. Opin. Solid State Mater. Sci.* **2004**, *8*, 111–120.

[24] It should be noted that the equipment used (see Experimental Section) does not allow the detection of pores with diameters lower than 2 nm.

[25] Because solid compounds have a higher susceptibility than fluid compounds, the spinning sidebands of solid compounds will be larger than the spinning sidebands of fluid components. Surface-affected components have broad peaks, whereas bulk fluid components have very sharp peaks. In the main peak, this broad peak cannot be distinguished from the sharp peak. In the spinning sidebands, however, the peak from the surface-affected phase will be higher due to the higher susceptibility.

[26] No NOE contacts were observed between the protons of TMB and any other component in the system. This might be due to the fact that TMB is very mobile and therefore has slow relaxation. In an attempt to decrease this mobility the temperature of the sample was lowered to 278 K; however, no NOE contacts could be observed between the CH and CH_3 protons of TMB and any other compound.

[27] R. M. E. Valckenborg, L. Pel, K. Kopinga, *J. Phys. D: Appl. Phys* **2002**, *35*, 249–256.

[28] K. Schmidt-Rohr and H. W. Spiess, *Multidimensional Solid-State NMR and Polymers*, Academic Press, London, **1994**.
[29] K. Schmidt-Rohr, J. Clauss, H. W. Spiess, *Macromolecules* **1992**, *25*, 3273–3277.
[30] P. L. Ritger, N. A. Peppas, *J. Controlled Release* **1987**, *5*, 23–36; N. A. Peppas, P. Bures, W. Leobandung, H. Ichikawa, *Eur. J. Pharm. Biopharm.* **2000**, *50*, 27–46.
[31] To minimize the amount of protons during synthesis, the HCl used in the synthesis was prepared by diluting a saturated HCl solution 12 times with D_2O; sodium silicate was also diluted four times with D_2O instead of with H_2O.
[32] S. J. Greg and K. S. W. Sing, *Adsorption, Surface Area and Porosity*, Academic Press, London, 2nd edn., **1995**.

Received: May 26, 2005
Revised: September 20, 2005
Published online: November 25, 2005

